

## Review article

## X-ray induced acoustic computed tomography

P. Samant<sup>b,c</sup>, L. Trevisi<sup>d</sup>, X. Ji<sup>a</sup>, L. Xiang<sup>e,\*</sup><sup>a</sup> School of Electromechanical Engineering, Guangdong University of Technology, Guangzhou, 510006, Guangdong, China<sup>b</sup> Stephenson School of Biomedical Engineering, University of Oklahoma, Norman, 73071, USA<sup>c</sup> Department of Oncology, University of Oxford, Oxford, OX3 7DQ, UK<sup>d</sup> Chemical, Biological, & Materials Engineering, University of Oklahoma, Norman, 73071, USA<sup>e</sup> Electrical and Computer Engineering, University of Oklahoma, Norman, 73071, USA

## ARTICLE INFO

## Keywords:

X-ray induced acoustic computed tomography  
 Radiation dosimetry  
 Low dose CT  
 Image guided therapy  
 Non-destructive testing  
 Density measurement  
 X-ray beam characterization

## ABSTRACT

X-ray imaging has proved invaluable in medical diagnoses and non-destructive testing (NDT) in the past century. However, there remain two major limitations: radiation harm and inaccessibility to the sample. A recent imaging modality, X-ray induced acoustic computed tomography (XACT), allows a novel solution. In XACT, x-ray induced excitation causes localized heating ( $< \text{mK}$ ) and thermoelastic expansion. This induces a detectable ultrasonic emission, thereby enabling imaging. XACT has the potential to enable low-dose, fast, 3D imaging requiring only single side access. We discuss the fundamentals of XACT and summarize milestones in its evolution over the past several years since its first demonstration using a Medical Linear Accelerator. We highlight XACT's potential applications in biomedical imaging and NDT, and discuss the latest advanced concepts and future directions.

## 1. Critical moments in X-ray history

X-ray imaging has made tremendous strides since its inception and has been widely deployed. However, during the long and successful history of x-ray imaging, certain limitations have persisted for more than a century. The first is that x-ray absorption-based images require placement of the x-ray detector opposite from the source. This can limit the applications of x-ray imaging in contexts where it is difficult to place a detector in the direct path of x-ray photons, for example, in the case of imaging large objects such as bridges or pavement. The second limitation is that ionizing radiation is in and of itself a carcinogen. As a result, x-ray applications in medical contexts must be balanced with the risk of large radiation doses applied to healthy tissues; in x-ray imaging, the minimization of radiation dose must be simultaneously balanced with the need to obtain high-quality images. In recent years, a novel x-ray imaging modality, x-ray induced acoustic computed tomography (XACT), has been emerging to overcome these limitations of conventional x-ray imaging. In this section we review the position of XACT relative to historical milestones in x-ray imaging.

As an X-ray imaging modality, XACT is best placed in context by briefly reviewing the history of X-ray research (Fig. 1). X-ray imaging has featured a wealth of research in the past  $\sim 130$  years. With its discovery in 1895 [1], a high level of interest in x-rays led to Wilhelm Roentgen being awarded the very first Nobel Prize in 1901. In 1913, following the development of the Coolidge tube [2], a wide variety of x-

ray applications were explored and realized by the scientific community. One of the most crucial breakthroughs in x-ray imaging, however, did not arrive until almost 60 years afterwards, when the work of Allan McLeod Cormack and Godfrey Hounsfield [3–6] led to the development of computed tomography (CT). Employing the mathematics of the Radon transform to generate 2D slice-by-slice images of any part of the human body, the CT scan was awarded the 1979 Nobel Prize in Physiology and Medicine (Fig. 1).

In 1983, the first acoustic signal generated by x-rays was demonstrated from a synchrotron source [7]. It was hypothesized that the acoustic source could emanate from a depth determined by the x-ray energy and the properties of the material itself. It was therefore suggested that x-ray generated ultrasound could provide information about the internal properties of materials. This was an important development towards addressing limitations of conventional x-ray imaging as x-ray induced ultrasound propagated in 3D, and so a detector did not necessarily have to be in the path of the x-ray photons. Additionally, as only a short-pulsed x-ray was required for the imaging, X-ray induced ultrasound had the potential to enable imaging with lower dose depositions as compared to conventional x-ray imaging.

Acoustic emission was also observed from a therapeutic x-ray source in 1991 [8], using an x-ray source, water absorber, and transducer arranged in such a way that an x-ray beam propagated perpendicular to the transducer head. Ultrasonic emissions were observed from the beam edges, with arrival times corresponding to the distance from the beam

\* Corresponding author at: 101 David L Boren Blvd Room 2022, Norman, 73071, USA.

E-mail address: [xianglzh@ou.edu](mailto:xianglzh@ou.edu) (L. Xiang).<https://doi.org/10.1016/j.pacs.2020.100177>

Received 13 November 2019; Received in revised form 10 March 2020; Accepted 10 March 2020

Available online 12 March 2020

2213-5979/ © 2020 The Author(s). Published by Elsevier GmbH. This is an open access article under the CC BY-NC-ND license (<http://creativecommons.org/licenses/by-nc-nd/4.0/>).

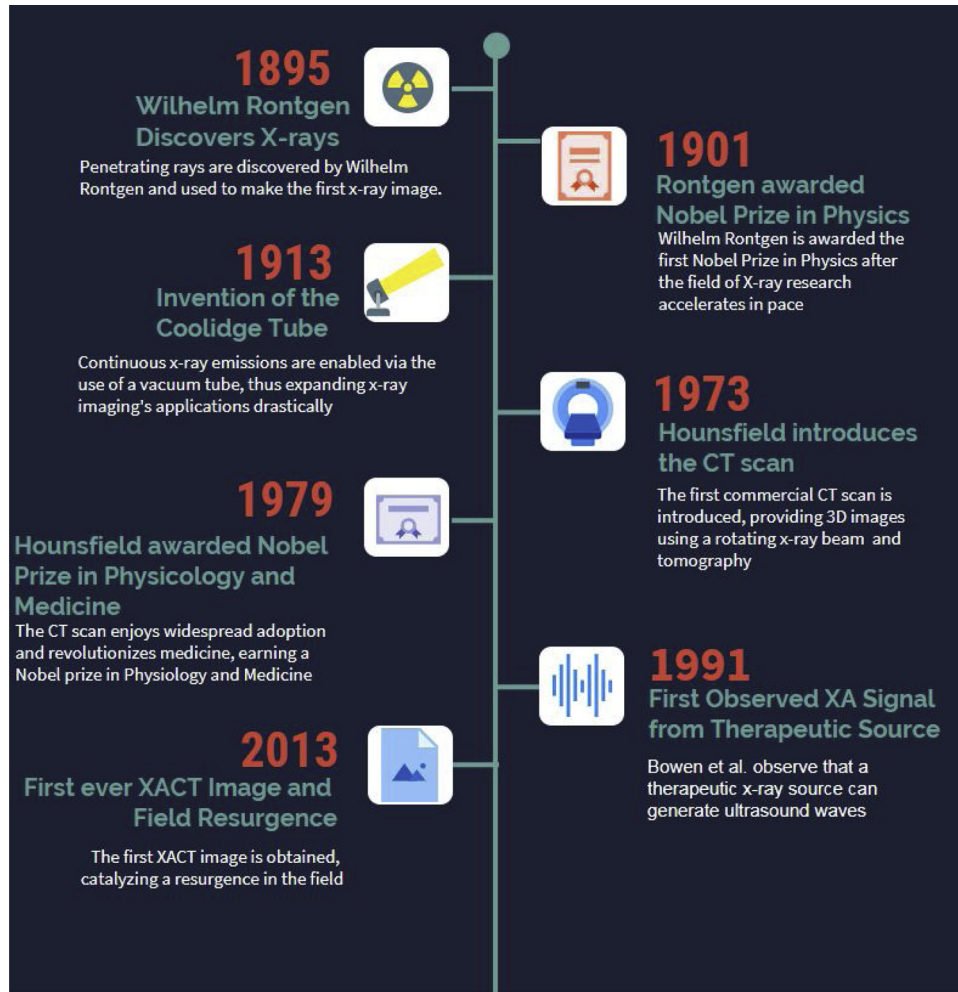


**Fig. 1.** Timeline of X-ray Imaging, discoveries in physics have enabled applications in medicine and NDT, typically on the time-scale of decades. XACT is now in a similar position following the detection of XA signals in 1991.

and the transducer. A 3400cGy corrected dose could produce a detectable signal 130 mm away from the beam. These experiments demonstrated that X-ray induced acoustic (XA) waves could be generated in clinical settings and showed that these XA waves could in turn encode information regarding the interaction of the absorbed x-rays with matter.

After initial work in the field in the 1980s and early 1990s, little research was done until 2013 when interest was rejuvenated, spurred on by technological advances in ultrasound transducers and the increasing complexity of pulsed X-ray sources. For the first time, x-ray induced acoustic signal has been used for tomographic imaging [9–12]. It was shown that short-pulsed 10 MV x-ray beams with dose rates of 30 Gy/min could generate acoustic signals that were detectable by a 500 kHz central frequency transducer driven by a computer-controlled step motor for scanning to achieve 2D imaging. A linear relationship between dose and the XA signal was also established and opens the possibility for its application of XACT imaging in radiation therapy monitoring. As this and many other new applications continue to be discovered, XACT continues to show potential in both non-destructive testing and medicine.

## 2. The X-ray induced acoustic effect

The mechanism through which X-rays can generate ultrasound is through photon-electron interactions (Fig. 2a). X-rays incident on the sample excite inner-shell electrons to generate photoelectrons, Auger

electrons, or electromagnetic radiation in the form of fluorescence. All three of these in turn impart thermal energy into the sample as fluorescence reabsorption, Auger electron absorption, and photoelectron absorption. Additionally, Compton scattering is also a major mechanism of energy deposition into the sample, and it is possible that Compton processes play a major role in x-ray energy deposition [13], however the exact details of the heat deposition mechanism from x-rays is not yet known. Nevertheless, these processes ultimately result in excited electrons depositing kinetic energy into the sample through electron-phonon interactions. This energy establishes as a small (mK) temperature rise in the sample, causing subsequent thermoelastic expansion and the emission of an acoustic wave in the ultrasound frequency range [8,14–17]. The X-ray induced Acoustic effect is a thermoacoustic phenomenon primarily governed by the following wave equation.

$$\left( \nabla^2 - \frac{1}{v_s^2} \frac{\partial^2}{\partial t^2} \right) p(\vec{r}, t) = -\frac{\beta}{C_p} \frac{\partial H(\vec{r}, t)}{\partial t} \quad (1)$$

Where  $p$  is the pressure as a function of position ( $\vec{r}$ ) and time ( $t$ ),  $v_s$  is the speed of sound in the medium,  $\beta$  is the coefficient of volume expansion,  $C_p$  is the specific heat capacity at constant pressure, and  $H$  is the heating function as a function of position and time (i.e. the absorbed power density). The heating function is typically known and is dependent primarily on the geometry of sample irradiation, whereas the pressure is typically unknown. The equation is driven by the first temporal derivative of the heating function itself, and therefore, time-

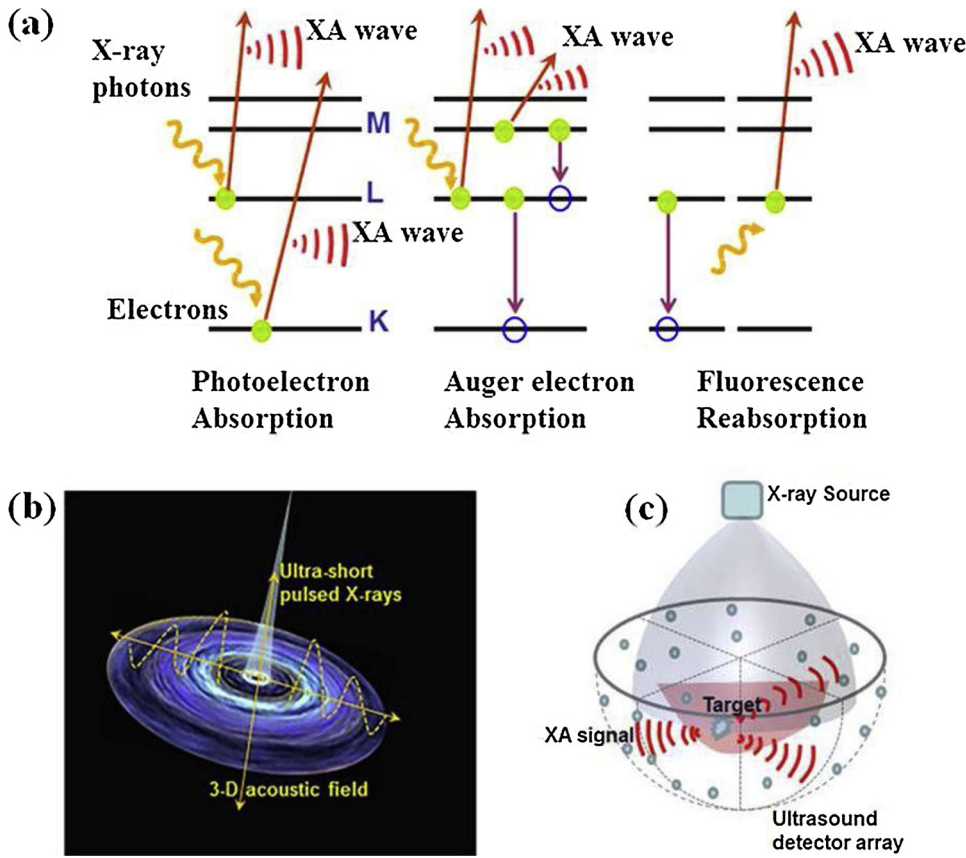


**Fig. 2.** Physics behind XACT. a) Electron interactions that lead to the production of XA signals, showing the role of photo electrons, Auger electrons, and Fluorescence processes. b) 3D acoustic fields are generated from ultra-short pulsed x-rays c) The generated acoustic field propagates in 3D. Figure reprinted with permission from Xiang et al. [18].

invariant heating will not produce an XA signal.

The heating, and therefore the irradiation, of the sample must be time-variant, ideally rapidly changing to maximize the derivative. It is for this reason that XACT systems and thermoacoustic systems employ pulsed excitation. The pressure wave produced in XACT travels in 3D from the point of excitation, and therefore can be detected by a 3D detector array (Fig. 2b,c).

To generate a strong acoustic signal, pressure must build up in the sample faster than it can propagate away for the duration of the acoustic excitation. This condition is known as stress confinement and it is met so long as the duration of the x-ray pulse,  $t_L$  is sufficiently small such that  $t_L < \frac{d_c}{v_s}$  where  $d_c$  is the characteristic length of heat heterogeneity in the sample (typically this is the desired resolution).<sup>14</sup> The initial pressure generated in the sample from an x-ray pulse depends on the dimensionless Grünesian parameter,  $\Gamma$ , of the sample at a given point, as well as the x-ray volumetric energy absorption (defined as energy absorbed per unit volume),  $A$ , of said sample. The initial pressure for a delta function excitation can then be written as [19]

$$p_0 = \Gamma A \quad (2)$$

$A$  is linked to the heating function through the integral relationship  $A(\vec{r}) = \int H(\vec{r}, t) dt$  [20]. The volumetric energy deposition can be expressed as the product of the fluence,  $F$ , and the x-ray energy absorption coefficient,  $\mu$ . The absorption coefficient and fluence can also be described in terms of the thermal efficiency (defined as the percentage of absorbed energy converted into heat),  $\eta_{th}$ , and the dose per pulse,  $D$  (defined as energy incident per unit mass). Then, Eq. 2 can be expressed in the following two forms [21]

$$p_0 = \Gamma \mu F = \Gamma \eta_{th} \rho D \quad (3)$$

Where  $\tau_p$  is the x-ray pulse duration,  $\rho$  is the mass density. It can be seen from Eq. 3 that the XA signal is directly proportional to the absorption coefficient of x-ray energy, the deposited dose into the sample, as well

as the mass density of the sample. This is one of the key physical properties of the XA signal that make it suited for a wide range of applications in biomedicine and NDT; contrast mechanisms of conventional x-ray imaging are retained, and the contrast information is encoded in a pressure wave that conveniently propagates at non-relativistic speeds in three dimensions. The physical characteristics of the XA signal continue to be a guiding mechanism through which additional applications of XACT can be explored going forward.

### 3. Applications

#### 3.1. Biomedical imaging

Biomedical applications of XACT range from diagnostic imaging in contexts such as conventional CT scans, and radiation oncology applications regarding therapy monitoring and radiation field characterization. The outlook of XACT in biomedical imaging is promising, as researchers work towards realizing a real-time *in-vivo* clinical XACT imaging system for therapy monitoring and imaging. In this section we present some of the key research directions of XACT in this biomedical imaging.

One of the first proposed applications of the XA effect is its potential employment in dosimetry and radiation therapy monitoring [10]. The XA signal is directly proportional to the energy deposited into the sample, and therefore, proportional to the radiation dose deposited in the sample [14,22,23]. This feature allows for XACT to yield real-time dosimetry information that can assist in radiation therapy monitoring and planning. End-to-end simulation workflows can model XACT's use for dosimetry and be validated with empirical study to optimize experimental parameters [24,25]. The already commonplace employment of Monte Carlo and treatment planning simulations in radiation therapy needs only to be coupled with additional simulations to model acoustic propagation. Since the initial pressure of the XA signal is directly

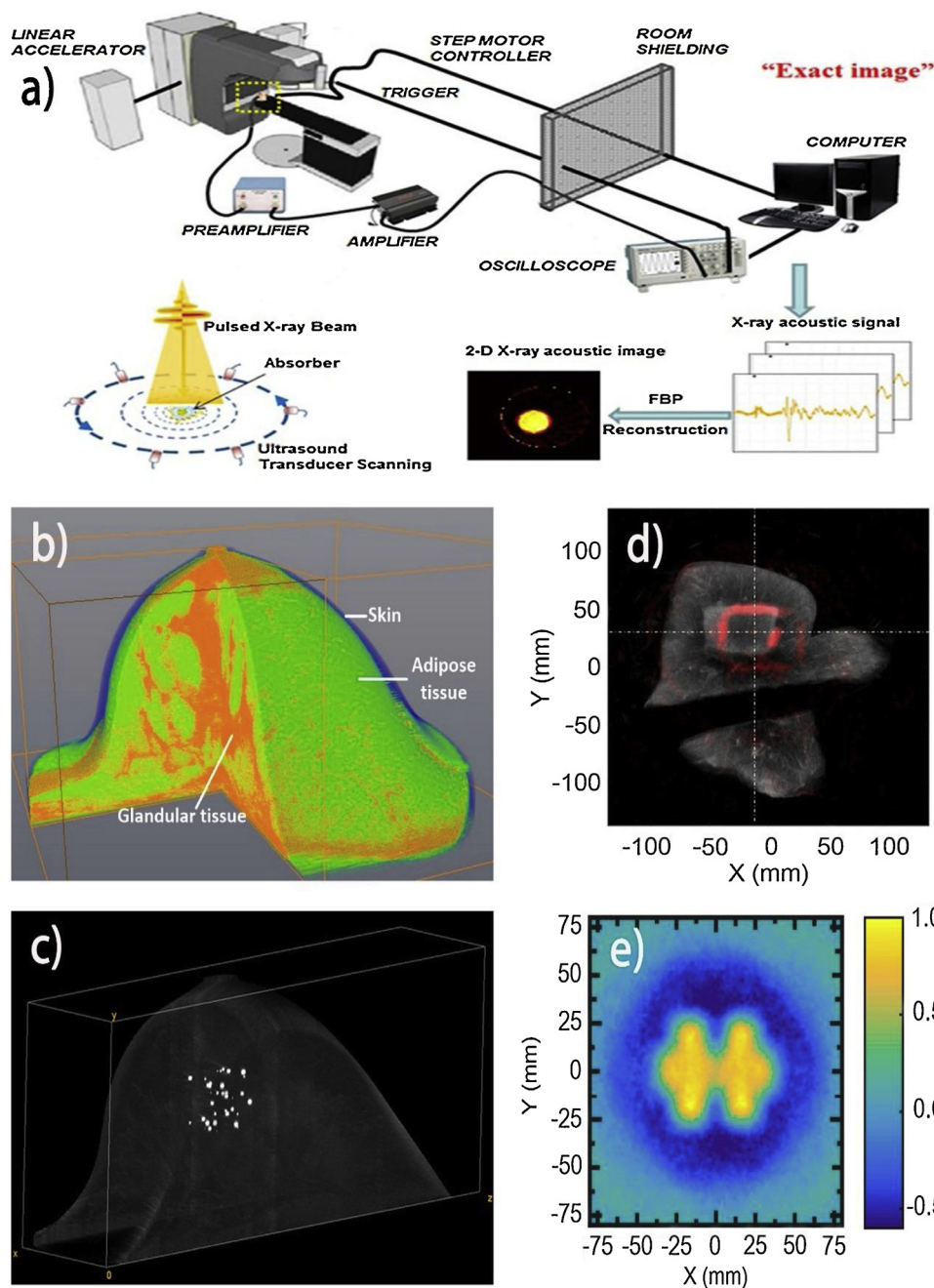


Fig. 3. a) Schematic of XACT, an x-ray source is directed to a sample and the subsequent XA signal is detected by a nearby transducer, the data is amplified and sent to a computer for processing. b) 3D breast volume rendering from segmentation results of 487 breast CT slices. c) 3D breast XACT volume showing the  $\mu$ Ca cluster. d) show the XACT image of the location of the beam overlapped with an ultrasonic image of a liver with a square of fat simulating a tumour. e) An experimental XACT image of a primary beam of a LINAC at 10 cm depth. Fig. 1 reprinted with permission from Robertson et al. Figures b,c reprinted with permission from Tang et al [32]. with the permission of AIP Publishing. Figure d reprinted with permission from Lei et al [33]. Figure e reprinted with permission from Hickling et al [34].

proportional to the beam energy, the output of Monte Carlo Simulations and treatment planning can be directly used as the input to acoustic models [24–26]. Experimental set-ups for XACT based dosimetry typically consist of a clinical Linac x-ray system for treatment, and a transducer. The transducer is placed near the beam and around the sample for acoustic detection (Fig. 3a). The detectors are acoustically coupled to the sample and placed close enough to the beam (without impeding it) such that acoustic attenuation is not a concern [18,27–31]. A pulse duration on the order of  $\mu$ s, as is commonplace with Linacs, will generate a million times weaker signal than a pulse of comparable energy lasting on the order of ns.

Nanosecond x-ray pulses are orders of magnitude more efficient at converting x-ray energy into an acoustic signal than microsecond pulsed used in Linacs [18,27–31]. Nevertheless, Linacs, having substantially higher energies than typically used nanosecond x-ray sources, have been repeatedly shown to produce detectable signals that have been confirmed to be proportional to x-ray dose [9,14,22,23,26,34–39].

Whereas early experiments on XACT typically involved the imaging of inorganic materials or those with high atomic number, more recently XACT signals have been detected from water [34]. Additionally, it was shown that XACT signals could be used in order to reconstruct dose distributions in water (Figs. 3e). XACT signals have also been detected in a real biological sample of veal liver (Fig. 3d), thereby providing experimental support for clinical translation of XACT [21]. Relative dose maps were well quantified in XACT, demonstrating both XACT's potential for dosimetry while providing an example of how XACT could be used for beam characterization. As clinical Linacs have been found to generate sufficiently large dose dependent XA signals, the implementation of clinical XACT dosimetry need not involve drastic changes to the radiation therapy process. The only required additions to clinical radiation therapy set-ups are an ultrasound transducer and a coupling medium. The radiation therapy procedure is otherwise unchanged, and so the adoption of XACT dosimetry in clinic does not require complicated additional steps beyond what is already practiced

in clinical settings.

Another application for XACT is radiological imaging. XACT imaging has been used to image Gold fiducial markers (GFM) with promising results for clinical translation potential [18]. GFMs are regularly employed in the clinic to better visualize and pinpoint the location of tumour tissue and register different imaging modalities [40–42], additionally, GFMs produce a strong XACT signal as compared to the background in biological samples. Therefore, high-resolution imaging of GFMs is an important research goal for clinical XACT. XACT imaging of GFMs showed resolutions as high as 0.35 mm in a prototype system, thereby demonstrating XACT's potential for high-resolution imaging comparable to micro-CT [18]. However, higher ultrasound resolutions are associated with higher ultrasound frequencies; high-resolution XACT imaging demands that the XA signal have high-frequency components present corresponding to the desired resolution. As higher thermoacoustic frequencies can be generated with shorter x-ray pulse durations, shortening the x-ray pulse can improve the resolution of XACT imaging. This is with the caveat that the bandwidth of the detecting transducer must be sufficiently high to detect generated signals, as signals with higher frequencies than the transducer bandwidth will not be detectable.

A major potential application of XACT is in mammography. XACT has the potential to address several issues facing x-ray based mammographic techniques. A common problem in the mammography of dense breasts remains that sensitivity decreases due to large tissue overlap, which manifests on the 2D mammographic image [43,44]. Therefore, 3D imaging is desirable in order to properly detect breast lesions early in these cases. Tang et al. proposed and simulated XACT imaging of the breast to classify microcalcifications, which can be a sign of early cancers in mammograms. The simulated x-ray source characteristics were 20 keV x-ray photon energy, an incident fluence of  $5.81\mu\text{J}/\text{cm}^2$ , and 60 ns pulse duration. Since XACT can be performed in 3D with a cup detector around the breast, the problem of tissue overlap present in dense breast mammography can be overcome via XACT implementation for breast imaging. While this can also be done with a dedicated breast CT or two-view mammography, XACT features a reduction in radiation dose as compared to either of these two modalities [32]. Simulation results of XACT breast imaging have been promising. Imaging a  $100\mu\text{m}$  diameter breast calcification in a 16 cm diameter breast phantom (Fig. 3b and 3c) was shown to result in a dose exposure as little as 0.36 mGy. For comparison, the average dose exposures of two-view digital mammography and screen-film mammography are 3.7 and 4.7 mGy, respectively [45]. This is a substantially lower dose (1/10th) than is typically delivered from mammography [32]. Additionally, lower pulse-widths generate higher frequencies, and therefore further dose reduction in XACT has the potential to yield both improved signal generation efficiency, as well as improve signal resolution. The noise equivalent pressure of this procedure was determined to be 1.65 mPa to ensure a signal to noise ratio of at least 4. The high-resolution imaging at low doses with high sensitivity bodes well for the future of XACT employment in breast imaging.

The biomedical applications of XACT include both biomedical imaging and radiation oncology through the introduction of high-resolution imaging techniques at low doses relative to CT imaging, and real-time monitoring of dose deposition in the body during radiation therapy for cancers. XACT has shown its potential towards imaging breast microcalcifications, gold fiducial markers, and dose depositions during radiation therapy. Through its versatile contrast mechanisms and fast imaging capabilities, the future of biomedical XACT is promising. The next step in biomedical XACT is its translation towards clinical practice.

### 3.2. Non-destructive testing

In recent years, XACT has found expanding applications outside of the context of biomedical imaging. Whereas the original imagined use

of XACT was for the analysis of biomedical structures, XACT can be extended towards various other contexts in which x-rays are typically used for assessment. One such direction is non-destructive testing (NDT) of both infrastructure and vehicles in industrial radiography. XACT has a unique advantage in these contexts as it requires access to only a single side of the sample. The primary methods through which general NDT of concrete is performed include electromagnetic techniques [46,47], stress wave techniques [48–56], radiography [57,58], and CT [59–61]. While all of these are applicable to concrete, all of them have some key limitations, such that XACT is uniquely poised to fill a role in NDT that other imaging modalities are not sufficient to do. Electromagnetic techniques require careful optimization for desired applications to maintain high imaging resolutions at appropriate depths, the same is true of acoustic techniques due to frequency attenuation, subsequently the resolution of both techniques is typically poor compared to x-ray modalities. CT and radiography offer superior resolution to either of these techniques. However, these x-ray modalities require placement of the x-ray detector in the path of incident x-rays, and so are not possible having access to only a single side of an object as is the case with acoustic and electromagnetic techniques. XACT, in contrast, can obtain resolutions comparably to CT and radiography while simultaneously offering convenient single side access offered by electromagnetic techniques. In this section we examine the potential of XACT for NDT applications.

The first study examining XACT's potential for NDT was relatively recent [62], but has nevertheless opened up a new application of XA signals for imaging. Aging and deteriorating infrastructure is a large problem in modern civil engineering, affecting power plants, bridges, roads, ports, airports, and buildings [63–65].

The assessment of these components often requires on-site measurements in order to estimate structure parameters such as integrity, quality, strength, and remaining lifetime. As XA signals propagate in all directions, XACT imaging of infrastructure requires only access to a single side. Signals originating from defects propagate right back toward the direction of the x-ray source. Here, they can be detected by a transducer and used to reconstruct an x-ray image using only single-side access, a schematic of this process is shown in Fig. 4a. This procedure is well modelled with the use of a numerical acoustic propagation model, which have previously been designed and implemented to simulate sub-pavement defect detection by a 3 MeV or 20 MeV x-ray photon energy source, with width of 30 cm, beam thickness of 1 mm, photon number of  $10^9$ , and pulse duration of  $20\mu\text{s}$  [62]. The resultant initial pressure from this procedure is shown in Fig. 4b after modelling pavement parameters and adding artificial defects. The presence of a linear transducer array was simulated, and the images were reconstructed to assess XACT potential for defect imaging. The result (Fig. 4c) shows that defects could be well imaged up to an imaging depth of 30 cm with center frequency of 150 kHz and 100 % bandwidth of transducers.

Simulations were also done of XACT imaging of the cross section of a 30 cm concrete bar with 4 rebars (1 damaged, 3 healthy) running along its length. The simulation geometry for this procedure is shown in Fig. 4d, a linear x-ray source is incident from the top of the page, illuminating the concrete bar and a square detection array immersed in a coupling medium. Fig. 4e shows a zoomed in section of the simulation showing the damaged rebar. The damaged rebar could be well visualized with XACT (Fig. 4f) after subtraction of an image of healthy rebars.

It can be seen from Fig. 4 that XACT was able to identify defects in both rebar localization contexts and sub-pavement concrete imaging contexts. Tang et al. also performed simulations on a 1 m diameter bridge column model and showed that XACT can characterize defects in this sample using a circular detection array.

Having demonstrated XACT potential for imaging of bridges, pavement, and rebars, Tang et al. were able to demonstrate the versatility and feasibility of XACT applications in the imaging of infrastructure. As the XA signal propagates in all direction, XACT can conveniently

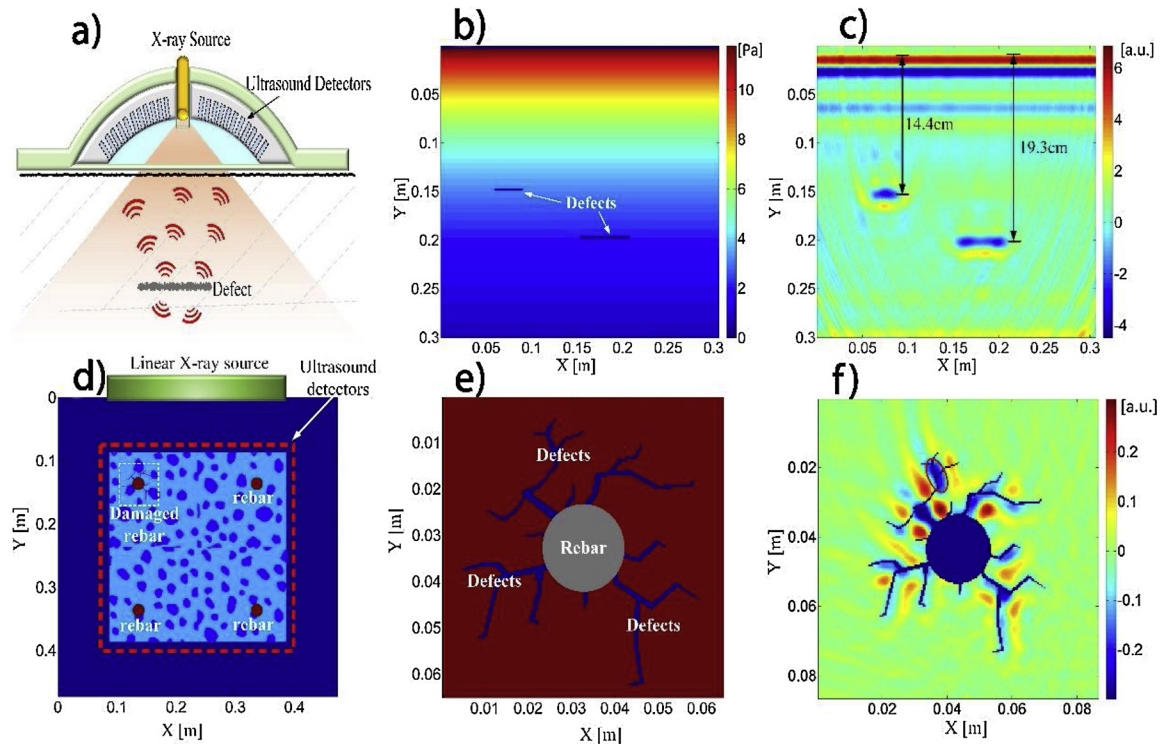


**Fig. 4.** XACT for NDT, demonstrating that pavement and rebar defects can be imaged. a) Schematic of XACT in this study b) initial pressure rise in the model, a linear transducer is along the top of the figure c) reconstructed XACT image of b, showing potential for sub-pavement defect detection and localization d) model for a cross section of a 30 cm concrete beam with embedded rebars, the top left rebar has a defect while the other three are healthy e) an enlarged view of the defected rebar f) the reconstructed enlarged view of e in simulation, showing the potential of XACT for rebar localization and sub-millimeter defect detection. Figure reproduced with permission from Tang et al [62].

provide x-ray absorption contrast imaging while requiring only single side access for infrastructure examination. Thus, a precedent has been set for XACT based NDT in a variety of large infrastructures.

## 4. Outlook

### 4.1. Potential of XACT

There are several key properties of XA signals that make them ideally suited for several different applications including but not limited

to what has been explored in literature. A road map of these applications is provided in Fig. 5. There are four key properties that make an XA signal ideally suited for various applications, 1) The XA signal amplitude is directly proportional to x-ray absorber density, 2) the XA signal amplitude is directly proportional to the deposited x-ray dose, 3) the XA wave propagates in 3D regardless of angle of the geometry of the x-ray excitation beam, 4) the XA signal requires only a short pulse of x-ray excitation for efficient signal generation. In this section, we discuss how the various physical properties of XA signals are useful in different applications.

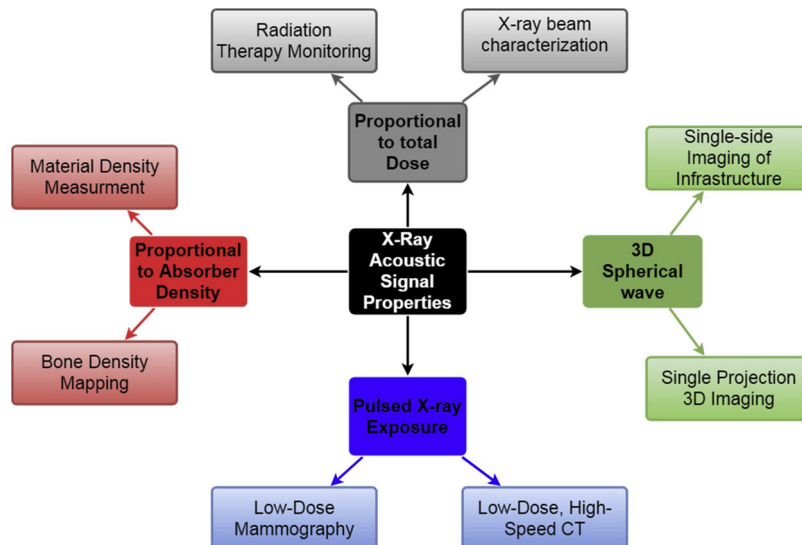


**Fig. 5.** Applications of XA Signal properties. Four key physical properties of the XA signal enable several research applications in Biomedicine and NDT.

The XA signal is proportional to the density of the absorber (Fig. 5, red), and therefore XACT imaging offers a potential method through which the density of materials and bones can be quantified in images. Areas of samples with higher density will in turn absorb more x-ray photons, and therefore produce strong X-ray signals. This means that, if desired, it is possible to achieve XACT imaging using density as a contrast mechanism, like dual energy CT for bone densitometry. This has important biomedical applications towards bone density mapping, as well as industrial applications for density determination and imaging of x-ray absorbing materials. However, quantitative imaging so far in XACT has not been achieved, as in the case of certain implementations of photoacoustic imaging (PAI) [66–69]; the development of quantitative image reconstruction algorithms remains an important future goal.

XA signal amplitudes are directly proportional to the total x-ray dose deposited in the sample (Fig. 5, grey). In the case of clinical radiation therapy, this feature enables a potential method to monitor and image dose distributions in target organs. As the dose is proportional to the acoustic signal, a map of the initial pressure reveals the relative dose distribution in tissue, which can be cross referenced with the location of the target organ in order to confirm beam alignment and accurate dose delivery [21]. Therefore, even though XACT imaging systems ultimately detect ultrasound, they nevertheless can use X-ray absorption as a contrast mechanism. For this reason, XACT has useful applications in the monitoring of dose deposition in radiation therapy. Especially, XACT imaging does not perturb the radiation beam because the transducers are placed outside of the beam path, eliminating the need for perturbation correction factors required by many other dosimetry techniques. In more specialized contexts such as x-ray laser research [21], the XA signal produced from beams can allow for the fine visualization of x-ray laser beam profiles for the context of alignment and optimization, which can also be extended to clinical beam profiling and characterization.

XA waves are 3D in nature (Fig. 5, green), and propagate in all directions from the point of generation. This allows for the volumetric x-ray imaging of samples with a single projection angle of the x-ray excitation source. The dimensionality of the imaging is limited only by the arrangement of detectors as opposed to the excitation source illumination; a 3D detector can produce a 3D image. This feature of the XA signals is also taken advantage of in the context of NDT. X-ray imaging for NDT applications typically requires the placement of detectors in the x-ray path after interaction with the sample. However, for large objects (e.g. airplane wings, bridges), this may not be feasible as only a single side is accessible. Therefore, X-ray imaging of large objects often requires the dismantling of said objects for imaging. XACT offers a solution to this problem, as the XA signal propagates in 3D, access to a single side of the object is sufficient for imaging; the detector can be placed on the same side on which the x-ray is incident. The 3D nature of XA signals therefore enables fast and convenient 3D imaging of samples. The XA signal is inversely proportional to the square of the pulse width of the x-ray. It is also directly proportional to the deposited energy. This is an important feature for dose reduction in XACT imaging as compared to conventional CT (Fig. 5, blue). Whereas the pulse duration and energy deposited are linearly related, the generated signal is proportional to the inverse square of the pulse width. Any effect of decreasing the beam energy on signal generation can be compensated for by decreasing the pulse width. The quadratic nature of the pulse width allows for the dose of XACT to be substantially lower than the dose of conventional CT [18]. XACT application for breast imaging yields a theoretical dose of 0.35 mGy, which is orders of magnitude smaller than that of typical images from dedicated breast CT imaging [18]. Moreover, recent research has shown that more rapid dose delivery (corresponding to shorter pulse duration) has the benefit of being less harmful to healthy tissue, presenting yet another potential benefit of XACT to patients [70–78]. The pulse relationship to the signal generation efficiency is a crucial XA signal property through which low-dose CT imaging of breast and other organs can be performed,

substantially lowering CT dose by using pulsed x-ray irradiation. Lastly, as in PAI, shorter pulse durations result in the generation of higher-frequency XA signals encoding higher resolution information.

The physical properties of XA signals have enabled several applications depending on the contexts in which the x-ray source and detector are deployed. The main applications so far are summarized in Fig. 5. The applications discussed in this letter range from biomedical applications and applications in NDT, ultimately these applications are driven by specific features of the physical XA signal.

#### 4.2. Challenges and future: fundamental limits

There are three underlying principles of XACT that act as fundamental limits on the modality: the characteristics of the x-ray source, the XA signal propagation before detection, and the ultrasonic detector characteristics. These must all be carefully considered when designing an XACT imaging system.

The x-ray source characteristics have a major impact on two main imaging components: the imaging depth and the imaging resolution. The maximum achievable imaging depth will always be fundamentally constrained by the penetration of x-rays through the sample of interest, with higher energy x-rays typically having higher penetration and therefore imaging depth. This means that the x-ray wavelength (and therefore source) should be carefully chosen depending on the sample of interest. Electron dense materials such as metals will require higher energy x-rays, whereas biological materials will require lower energy x-rays. The penetration of x-rays must also be balanced with the absorption, as enough energy must be deposited into the sample to generate a strong XA signal. In the case of biomedical imaging, the x-ray energy should be balanced with the need to minimize dose to patients. As in PAI, there is a depth vs. resolution trade-off in XACT imaging, and therefore higher imaging depth typically comes at the cost of lower resolution and vice versa.

It is to be noted that the generation of XA waves is due to rapid changes in the illumination intensity, i.e. it is important to ensure that the temporal derivative of the x-ray intensity is maximized. In the case of Gaussian x-ray pulse sources, this amounts to keeping the pulse duration sufficiently short. As in PAI, higher XA frequencies are generated by shorter pulse durations, which correspond to higher imaging resolutions. Therefore, the x-ray pulse duration must be sufficiently short to generate signals in the frequency range that corresponds to the desired imaging resolution. Consequently, for both the purposes of SNR and resolution optimization, the pulse width of the x-ray source must be chosen very carefully depending on imaging goals.

The XA signal must be allowed to propagate through the sample and arrive at the detector with minimal attenuation. Ultimately this means that samples with large acoustic impedance variances will be very difficult to image in. However, so long as large parts of the sample are impedance matched (as is often the case when imaging soft tissue and samples in NDT), the x-ray signal should propagate with minimal scattering. This means that in contexts such as aircraft wing and concrete imaging for NDT, the irradiation area must be acoustically coupled with the detector, which is important to consider when planning the irradiation geometry and transducer placement. The XA signal is also subject to frequency attenuation (higher frequencies cannot travel as far in media) and amplitude attenuation as it propagates through the sample. As in PAI, higher XA frequencies are attenuated more than lower frequencies as they travel through the sample, which leads to the resolution-imaging depth trade-off in imaging. In order to minimize the effect of ultrasonic absorption and frequency attenuation, the distance between the transducer and source should be minimized. This is especially important when high-resolutions are desired.

Finally, as the signal propagates to the sensors, it must be strongly detected to be converted into a voltage. This places several fundamental limits on the sensors themselves which must be considered in all XACT implementations. The frequency response of the sensors must be well

matched to the frequency spectrum of the arriving signal, otherwise sensitivity of the system and resolution of the reconstructed image will suffer.

#### 4.3. Challenges and future: implementation

There are several future research goals that have yet to be achieved towards biomedical and NDT oriented XACT. In this section we discuss some of the key engineering challenges left to overcome in XACT as well as future goals of the field.

It must be assured, when choosing a transducer and coupling material, that the ultrasonic signal has an impedance matched path to the transducer with minimal attenuation. Therefore, it is typically desirable to minimize the distance from the source and the transducer when seeking higher resolution and higher SNR. Additionally, the material of both the wiring and the transducer must be able to withstand longitudinal exposure to x-ray radiation. However, it not yet known how such exposure may affect ultrasonic equipment with high ionizing radiation doses present, and special consideration must be taken to ensure radiation endurance. It is important to investigate these potential effects and the need for shielding prior to clinical translation of XACT, this remains an open question currently. While there have not yet been any studies on the long-term transducer performance effects caused by exposure to pulsed x-ray radiation, it is a well documented phenomenon that x-ray radiation creates a temporary voltage rise immediately after firing [28]. It is currently believed that this temporary voltage transient is due to electrical noise caused by scattered x-rays producing a signal on the transducer surface. While the transient is large in amplitude and therefore has the potential to disrupt XACT signal collection, it is short lasting and can be removed from the signal by excluding data taken immediately (typically on the order of single  $\mu$ s) after the firing of the x-ray. Further investigation of the cause of this transient is also necessary to verify its cause.

Currently all research modelling XA signal propagation in tissue has been done through the k-wave MATLAB toolbox [26,32,62,79,80]. If X-ray absorption also needs to be modelled for complex geometries, then it is also important to note that separate Monte Carlo simulations will be necessary in order to accurately model the x-ray energy deposition in the sample.

XACT imaging dimensionality is largely dependent on the type of array that can be deployed. In general, at least a 2D array must be deployed in order to achieve 3D imaging without the need for scanning. The manufacture of such arrays is a major challenge in XACT, as the array must have the appropriate bandwidth, sensitivity, number of detectors, sampling rate, and directionality to detect the XA signal, which is typically very weak. Of these the most challenging part is the maximization of the number of detectors (and the accompanying high channel count). Additionally, auxiliary electronics (e.g. filters and amplifiers) must also be developed with the array to enable signal detection at suitable SNRs. This is one of the most important problems in XACT imaging today. So far, ring array based detection [81] has been demonstrated in XACT, albeit requiring extensive averaging ( $\sim 2000$  times) in order to achieve strong SNRs, this system can be improved upon via the addition of a preamplification system in order to enable high SNR 2D XACT without the need for extensive averaging. Cup detectors and 3D arrays have not yet been successfully deployed for 3D XACT imaging, however manufacture of such arrays can borrow methodology already developed in the field of PAI [82–85] in order to hasten 3D XACT imaging development. The development of appropriate arrays, amplification, and filtering systems for XACT is the most important engineering challenge in this field.

Real-time imaging is one of the potential advantage of XACT over conventional CT imaging. This is because with a single pulse, XACT provides a 3D signal. Therefore it is possible to generate a 2D or 3D image with a single pulse, which speeds up data collection considerably. If the rapidly collected data can be combined with a fast

reconstruction algorithm, then such an optimized XACT is capable of real-time imaging. The primary challenge to overcome in this context is the acquisition of a sufficiently high signal-to-noise ratio (SNR) such that averaging of the XA signal is not necessary. For this to be achieved, the XA pulse must be well characterized to optimize filtering of detected signals, and amplification of multiple channels must be enabled to as to provide high SNR in all elements of an imaging array. The development of 3D image reconstruction algorithms specific to transducer array geometries is also necessary for the realization of fast 3D XACT imaging, specifically algorithms that can solve the limited view problem are of particular interest [21]. Studies so far have been limited to imaging using a single transducer scanned with a step motor or using an ultrasonic 2D ring array.

Quantitative imaging so far in XACT has not been achieved, as in the case of certain implementations of PAI [66–68]. Reconstruction algorithms specific to transducer and source geometry have the potential to yield detailed and accurate dose maps and radiation field characterization when coupled with experimental results [22,86,87], however the research in this area of XACT is still in its infancy. Recently, it has been suggested that the deployment of iterative reconstruction algorithms could enable absolute dosimetry in XACT [79], but research is ongoing.

The realization of a clinical XACT system is also an important milestone that has yet to be achieved [27,80,87–89,89–92]. There remain several topics on which more research is required as well as additional experimental milestones that much first be reached before this is a reality. Further research is needed on an x-ray source for the imaging of structures as small as microcalcifications, as current clinical Linacs typically operate at pulse widths in the microsecond range, too long for sub-mm resolutions. Additionally, it must be demonstrated that a strongly detectable XACT signal is possible from human tissue phantoms, whereas XA signals have been detected from medical Linacs from fat tissue, detection of XA waves in clinical settings has yet to be achieved [93].

Whereas simulations have been encouraging, the use of XACT in NDT is a young idea, with the first paper on the subject just released in 2018. The next step towards industrial employment of XACT for infrastructure defect detection is the experimental detection of an XA signal from a concrete sample. Research in obtaining empirical support for XACT NDT applications is ongoing. A suitable reconstruction algorithm will also need to be developed in addition to more accurate simulation software.

Currently, there is very little research on dedicated reconstruction modalities for XACT. The work that has been done so far typically implements time reversal reconstruction (assume acoustic homogeneity) using the k-wave toolbox, or uses filtered back-projection reconstruction algorithms [81,87,94]. Neither of these reconstruction methods account for acoustic heterogeneities, which presents a major challenge for XACT implementation *in vivo*. Fortunately, there is a wealth of research in solving these problems within the field of photoacoustics [95–99], and therefore there exist several methods from laser-induced PAI that could be borrowed in order to enable XACT image reconstruction in the presence of acoustic heterogeneities. The main challenge in heterogeneous reconstruction is the lack of knowledge *a priori* of the sound speed distribution, and so the deployment of other imaging modalities (such as conventional ultrasound, conventional x-ray imaging) could be combined with XACT in contexts where this distribution is necessary to know. Additionally, there are families of algorithms that can account for heterogeneous reconstruction.

An especially promising algorithm family for translation from PAI to XACT is that of iterative reconstruction, which could enable 3D imaging while accounting for acoustic heterogeneities [95,96]. Additionally, for extraction of information such as density and x-ray absorption coefficient, algorithms from quantitative PAI can be deployed [67,100,101], however more research about the specific implementation of these techniques to XACT is needed. The translation of these techniques from

PAI to XACT is a direction of future research, and offers promise to solve the problems of both quantitative imaging as well as heterogeneity correction.

In summary, XACT remains a young field, but is currently in the process of experiencing a rapid growth in interest. Due to its versatile contrast mechanisms, combined with low-dose, fast, 3D imaging capabilities requiring single side access to the sample, XACT has the potential to revolutionize the use of x-rays in biomedicine and NDT. Though a relatively new field, interest in XACT as undergone an exponential increase in the past years. XACT imaging exploits the nature of XA signals, to enable multiple imaging setups for uses in broad applications. The future of XACT is bright as more applications continue to be studied through simulations and realized through experiments.

### Declaration of Competing Interest

The authors declare that they have no conflicts of interest related to this manuscript.

### Acknowledgements

This work was partially supported by the Guangdong Innovative and Entrepreneurial Research Team Program (Grant No. 2016ZT06G375), National Science Foundation Grants (NSFC Grant No. 51975131) to Dr. Xuanrong Ji. This work was also partially supported by National Institute of Health (R37CA240806), American Cancer Society (133697-RSG-19-110-01-CCE), and the Oklahoma Center for the Advancement of Science and Technology (HR19-131) to Dr. Liangzhong Xiang. The authors would like to acknowledge the support from Stephenson Cancer Center bridge fund, IBEST-OUHSC fund, and a grant from the Research Council of the University of Oklahoma Norman Campus as well.

### References

- [1] W.C. Röntgen, On a new kind of rays, *Science* 3 (1896) 227–231, <https://doi.org/10.1126/science.3.59.227>.
- [2] W.D. Coolidge, A powerful Röntgen Ray Tube with a pure Electron discharge, *Phys. Rev.* 2 (1913) 409–430, <https://doi.org/10.1103/PhysRev.2.409>.
- [3] G.N. Hounsfield, Computerized transverse axial scanning (tomography): part 1. Description of system, *BJR* 46 (1973) 1016–1022, <https://doi.org/10.1259/0007-1285-46-552-1016>.
- [4] G.N. Hounsfield, A method of and apparatus for examination of a body by radiation such as X or gamma-radiation, British Patent No. 1,283,915. (1972). <http://ci.nii.ac.jp/naid/10014659449/> (Accessed July 2, 2018).
- [5] A.M. Cormack, Representation of a function by its line integrals, with some radiological applications, *J. Appl. Phys.* 34 (1963) 2722–2727, <https://doi.org/10.1063/1.1729798>.
- [6] A.M. Cormack, Representation of a function by its line integrals, with some radiological applications, II, *J. Appl. Phys.* 35 (1964) 2908–2913, <https://doi.org/10.1063/1.1713127>.
- [7] K.Y. Kim, W. Sachse, X-ray generated ultrasound, *Appl. Phys. Lett.* 43 (1983) 1099–1101, <https://doi.org/10.1063/1.94240>.
- [8] T. Bowen, C.X. Chen, S.C. Liew, W.R. Lutz, R.L. Nasoni, Observation of ultrasonic emission from edges of therapeutic X-ray beams, *Phys. Med. Biol.* 36 (1991) 537, <https://doi.org/10.1088/0031-9155/36/4/011>.
- [9] L. Xiang, B. Han, C. Carpenter, G. Pratz, Y. Kuang, L. Xing, X-ray acoustic computed tomography with pulsed x-ray beam from a medical linear accelerator, *Med. Phys.* 40 (2013) 010701, <https://doi.org/10.1118/1.4771935>.
- [10] L. Xiang, B. Han, C. Carpenter, G. Pratz, Y. Kuang, L. Xing, X-ray induced photoacoustic tomography, *Photons Plus Ultrasound: Imaging and Sensing 2013*, International Society for Optics and Photonics (2013) 858111, <https://doi.org/10.1117/12.2005765>.
- [11] L. Xiang, M. Ahmad, A. Nikoozadeh, G. Pratz, B. Khuri-Yakub, L. Xing, TU-A-9A-07: X-Ray Acoustic Computed Tomography (XACT): 100% Sensitivity to X-Ray Absorption, *Med. Phys.* 41 (2014), <https://doi.org/10.1118/1.4889242> 448–448.
- [12] L. Xiang, M. Ahmad, C. Carpenter, G. Pratz, A. Nikoozadeh, B. Khuri-Yakub, L. Xing, TH-a-141-02: X-Ray acoustic computed tomography: concept and design, *Med. Phys.* 40 (2013), <https://doi.org/10.1118/1.4815707> 522–522.
- [13] X.M. Tong, H. Yamaoka, H. Nagasawa, T. Watanabe, Heat-energy deposition in x-ray interaction with materials application to Si and Be, *J. Appl. Phys.* 78 (1995) 2288–2297, <https://doi.org/10.1063/1.360146>.
- [14] S. Hickling, Feasibility of x-ray Acoustic Computed Tomography As a Relative and in Vivo Dosimeter in Radiotherapy Applications, McGill University, 2015, <http://oatd.org/oatd/record?record=oai%5C%3Adigitool.library.mcgill.ca%5C%3A130671>.
- [15] M.E. Garcia, G.M. Pastor, K.H. Bennemann, Theory for the photoacoustic response to X-Ray absorption, *Phys. Rev. Lett.* 61 (1988) 121–124, <https://doi.org/10.1103/PhysRevLett.61.121>.
- [16] Y. Fang, A.N. Vasil'ev, V.V. Mikhailin, Theory of X-ray photoacoustic spectroscopy, *Appl. Phys. A* 60 (1995) 333–341, <https://doi.org/10.1007/BF01538414>.
- [17] W. Assmann, S. Kellnberger, S. Reinhardt, S. Lehrack, A. Edlich, P.G. Thirolf, M. Moser, G. Dollinger, M. Omar, V. Ntziachristos, K. Parodi, Ionoacoustic characterization of the proton Bragg peak with submillimeter accuracy, *Med. Phys.* 42 (2015) 567–574, <https://doi.org/10.1118/1.4905047>.
- [18] L. Xiang, S. Tang, M. Ahmad, L. Xing, High resolution X-ray-Induced acoustic tomography, *Sci. Rep.* 6 (2016) 26118, <https://doi.org/10.1038/srep26118>.
- [19] L.V. Wang, Tutorial on photoacoustic microscopy and computed tomography, *IEEE J. Sel. Top. Quantum Electron.* 14 (2008) 171–179, <https://doi.org/10.1109/JSTQE.2007.913398>.
- [20] L.V. Wang, Tutorial on photoacoustic microscopy and computed tomography, *IEEE J. Sel. Top. Quantum Electron.* 14 (2008) 171–179, <https://doi.org/10.1109/JSTQE.2007.913398>.
- [21] H. Lei, W. Zhang, I. Oraiqat, Z. Liu, J. Ni, X. Wang, I. El Naqa, Toward in vivo dosimetry in external beam radiotherapy using x-ray acoustic computed tomography: a soft-tissue phantom study validation, *Med. Phys.* (2018), <https://doi.org/10.1002/mp.13070>.
- [22] S. Hickling, M. Hobson, I.E. Naqa, Feasibility of X-Ray acoustic computed tomography as a tool for noninvasive volumetric in vivo dosimetry, *Int. J. Radiat. Oncol. Biol. Phys.* 90 (2014) S843, <https://doi.org/10.1016/j.ijrobp.2014.05.2417>.
- [23] Hickling Susannah, Lei Hao, Hobson Maritza, Pierre Leger, Xueding Wang, Naqa Issam El, Sci-Thur AM: YIS – 02: Imaging dose distributions through the detection of radiation-induced acoustic waves, *Med. Phys.* 43 (2016), <https://doi.org/10.1118/1.4961751> 4928–4928.
- [24] B.E. Treeby, B.T. Cox, k-Wave: MATLAB toolbox for the simulation and reconstruction of photoacoustic wave fields, *J. Biomed. Opt.* 15 (2010) 021314, <https://doi.org/10.1117/1.3360308>.
- [25] B.E. Treeby, J. Jaros, D. Rohrbach, B.T. Cox, Modelling elastic wave propagation using the k-wave MATLAB toolbox, 2014 IEEE International Ultrasonics Symposium (2014) 146–149, <https://doi.org/10.1109/ULTSYM.2014.0037>.
- [26] S. Hickling, P. Léger, I.E. Naqa, Simulation and experimental detection of radiation-induced acoustic waves from a radiotherapy linear accelerator, 2014 IEEE International Ultrasonics Symposium (2014) 29–32, <https://doi.org/10.1109/ULTSYM.2014.0008>.
- [27] R. Faiz, S. Tang, B. Zheng, H. Liu, A. Zafarshani, L. Xiang, Fast X-ray-induced acoustic computed tomography, *Med. Phys.* 44 (2017) (accessed March 26, 2018), <https://insights-ovid-com.ezproxy.lib.ou.edu/medical-physics/medph/2017/06/000/fast-ray-induced-acoustic-computed-tomography/2450/00005706>.
- [28] S. Tang, D.H. Nguyen, A. Zafarshani, C. Ramseyer, B. Zheng, H. Liu, L. Xiang, X-ray-induced acoustic computed tomography with an ultrasound transducer ring-array, *Appl. Phys. Lett.* 110 (2017) 103504, <https://doi.org/10.1063/1.4978049>.
- [29] S. Tang, L. Ren, P. Samant, J. Chen, H. Liu, L. Xiang, Sub-mSV breast XACT scanner: concept and design, *Medical Imaging 2016: Ultrasonic Imaging and Tomography*, International Society for Optics and Photonics (2016) 97900L, <https://doi.org/10.1117/12.2211079>.
- [30] S. Tang, Y. Chen, J. Chen, P. Samant, S. Ahmad, H. Liu, L. Xiang, TH-AB-209-08: Next Generation Dedicated 3D Breast Imaging with XACT, *Med. Phys.* 43 (2016), <https://doi.org/10.1118/1.4958099> 3865–3865.
- [31] S. Tang, Y. Chen, S. Ahmad, K. Yang, R. Laaroussi, J. Chen, P. Samant, L. Xiang, SU-F-I-14: 3D Breast Digital Phantom for XACT Imaging, *Med. Phys.* 43 (2016), <https://doi.org/10.1118/1.4955842> 3389–3389.
- [32] S. Tang, K. Yang, Y. Chen, L. Xiang, X-ray induced acoustic computed tomography for 3D breast imaging: a simulation study, *Med. Phys.* (2018), <https://doi.org/10.1002/mp.12829>.
- [33] W. Zhang, H. Lei, I. Oraiqat, I.E. Naqa, X. Wang, Real-time monitoring the alignment of x-ray beam relative to treatment target during radiation treatment based on ultrasound and x-ray acoustic dual-modality imaging (Conference presentation), *Photons Plus Ultrasound: Imaging and Sensing 2018*, International Society for Optics and Photonics (2018) 104940E, <https://doi.org/10.1117/12.2289107>.
- [34] S. Hickling, H. Lei, M. Hobson, P. Léger, X. Wang, I. El Naqa, Experimental evaluation of x-ray acoustic computed tomography for radiotherapy dosimetry applications, *Med. Phys.* 44 (2016) 608–617, <https://doi.org/10.1002/mp.12039>.
- [35] X. Diao, J. Zhu, W. Li, N. Deng, C.T. Chin, X. Zheng, X. Zhang, X. Chen, X. Li, Y. Kuang, Broadband detection of dynamic acoustic emission process induced by 6 MV therapeutic X-ray beam from a clinical linear accelerator, 2015 IEEE International Ultrasonics Symposium (IUS) (2015) 1–4, <https://doi.org/10.1109/ULTSYM.2015.0241>.
- [36] S. Hickling, M. Hobson, I.E. Naqa, Characterization of x-ray acoustic computed tomography for applications in radiotherapy dosimetry, *IEEE Trans. Radiat. Plasma Med. Sci.* PP (2018), <https://doi.org/10.1109/TRPMS.2018.2801724> 1–1.
- [37] S. Hickling, P. Léger, I.E. Naqa, On the detectability of acoustic waves induced following irradiation by a radiotherapy linear accelerator, *IEEE Trans. Ultrason. Ferroelectr. Freq. Control* 63 (2016) 683–690, <https://doi.org/10.1109/TUFFC.2016.2528960>.
- [38] S. Hickling, M. Hobson, I. El Naqa, MO-A-BRD-07: feasibility of X-ray acoustic computed tomography as a tool for calibration and in vivo dosimetry of radiotherapy electron and photon beams, *Med. Phys.* 41 (2014), <https://doi.org/10.1118/1.4889110> 409–409.

- [39] J. Kim, E.Y. Park, Y. Jung, B.C. Kim, J.H. Kim, C.Y. Yi, I.J. Kim, C. Kim, X-ray acoustic-based dosimetry using a focused ultrasound transducer and a medical linear accelerator, *IEEE Trans. Radiat. Plasma Med. Sci.* 1 (2017) 534–540, <https://doi.org/10.1109/TRPMS.2017.2757484>.
- [40] D.J. Moseley, E.A. White, K.L. Wiltshire, T. Rosewall, M.B. Sharpe, J.H. Siewersden, J.-P. Bissonnette, M. Gospodarowicz, P. Warde, C.N. Catton, D.A. Jaffray, Comparison of localization performance with implanted fiducial markers and cone-beam computed tomography for on-line image-guided radiotherapy of the prostate, *Int. J. Radiat. Oncol.* 67 (2007) 942–953, <https://doi.org/10.1016/j.ijrobp.2006.10.039>.
- [41] H. Shirato, T. Harada, T. Harabayashi, K. Hida, H. Endo, K. Kitamura, R. Onimaru, K. Yamazaki, N. Kurauchi, T. Shimizu, N. Shinohara, M. Matsushita, H. Dosaka-Akita, K. Miyasaka, Feasibility of insertion/implantation of 2.0-mm-diameter gold internal fiducial markers for precise setup and real-time tumor tracking in radiotherapy, *Int. J. Radiat. Oncol.* 56 (2003) 240–247, [https://doi.org/10.1016/S0360-3016\(03\)00076-2](https://doi.org/10.1016/S0360-3016(03)00076-2).
- [42] J.M. Schallenkamp, M.G. Herman, J.J. Kruse, T.M. Pisansky, Prostate position relative to pelvic bony anatomy based on intraprostatic gold markers and electronic portal imaging, *Int. J. Radiat. Oncol.* 63 (2005) 800–811, <https://doi.org/10.1016/j.ijrobp.2005.02.022>.
- [43] A.M. O'Connell, A. Karellas, S. Vedantham, The potential role of dedicated 3D breast CT as a diagnostic tool: review and early clinical examples, *Breast J.* 20 (2014) 592–605, <https://doi.org/10.1111/tbj.12327>.
- [44] X. Qin, G. Lu, I. Sechopoulos, B. Fei, Breast tissue classification in digital tomosynthesis images based on global gradient minimization and texture features, *Medical Imaging 2014: Image Processing*, International Society for Optics and Photonics (2014), <https://doi.org/10.1117/12.2043828> p. 90341V.
- [45] R.E. Hendrick, Radiation doses and Cancer risks from breast imaging studies, *Radiology* 257 (2010) 246–253, <https://doi.org/10.1148/radiol.10100570>.
- [46] A. Buttress, A. Jones, S. Kingman, Microwave processing of cement and concrete materials – towards an industrial reality? *Cem. Concr. Res.* 68 (2015) 112–123, <https://doi.org/10.1016/j.cemconres.2014.11.002>.
- [47] S.N. Jammalamadaka, G. Markandeyulu, E. Kannan, K. Balasubramaniam, Development of a magnetostriuctive transducer for nondestructive testing of concrete structures, *Appl. Phys. Lett.* 92 (2008) 044102, <https://doi.org/10.1063/1.2834368>.
- [48] M. Krause, M. Bärmann, R. Frielinghaus, F. Kretschmar, O. Kroggel, K.J. Langenberg, C. Maierhofer, W. Müller, J. Neisecke, M. Schick, V. Schmitz, H. Wiggenhauser, F. Wollbold, Comparison of pulse-echo methods for testing concrete, *Ndt E Int.* 30 (1997) 195–204, [https://doi.org/10.1016/S0963-8695\(96\)00056-4](https://doi.org/10.1016/S0963-8695(96)00056-4).
- [49] C. Cheng, M. Sansalone, The impact-echo response of concrete plates containing delaminations: numerical, experimental and field studies, *Mater. Struct.* 26 (1993) 274–285, <https://doi.org/10.1007/BF02472949>.
- [50] C.-Y. Wang, S.-T. Liao, J.-H. Tong, C.-L. Chiu, Numerical and experimental study on multi-directional SAFT to detect defects inside plain or reinforced concrete, *Constr. Build. Mater.* 76 (2015) 351–359, <https://doi.org/10.1016/j.conbuildmat.2014.12.018>.
- [51] S. Beniwal, A. Ganguli, Defect detection around rebars in concrete using focused ultrasound and reverse time migration, *Ultrasonics* 62 (2015) 112–125, <https://doi.org/10.1016/j.ultras.2015.05.008>.
- [52] T. Ju, J.D. Achenbach, L.J. Jacobs, M. Guimaraes, J. Qu, Ultrasonic nondestructive evaluation of alkali-silica reaction damage in concrete prism samples, *Mater. Struct.* 50 (2017) 60, <https://doi.org/10.1617/s11527-016-0869-6>.
- [53] Y.S. Cho, Non-destructive testing of high strength concrete using spectral analysis of surface waves, *NDT & E Int.* 36 (2003) 229–235, [https://doi.org/10.1016/S0963-8695\(02\)00067-1](https://doi.org/10.1016/S0963-8695(02)00067-1).
- [54] I.N. Prassianakis, E. Sideridis, A. Vamvakousis, The Characterisation of Old Concrete Using Destructive and the Ultrasonic Non-destructive Testing Methods, (2003), <https://doi.org/10.1784/insi.45.12.827.52985>.
- [55] H. Choi, J.S. Popovics, NDE application of ultrasonic tomography to a full-scale concrete structure, *IEEE Trans. Ultrason. Ferroelectr. Frequency Control* 62 (2015) 1076–1085, <https://doi.org/10.1109/TUFFC.2014.006962>.
- [56] I.N. Prassianakis, E. Sideridis, A. Vamvakousis, The Characterisation of Old Concrete Using Destructive and the Ultrasonic Non-destructive Testing Methods, (2003), <https://doi.org/10.1784/insi.45.12.827.52985>.
- [57] A.A. Naqvi, M. Maslehuddin, Z. Kalakada, O.S.B. Al-Amoudi, Prompt gamma ray analysis for chlorine analysis in blended cement concrete, *Appl. Radiat. Isot.* 94 (2014) 8–13, <https://doi.org/10.1016/j.apradiso.2014.06.011>.
- [58] A. Sarapata, M. Ruiz-Yaniz, I. Zanette, A. Rack, F. Pfeiffer, J. Herzen, Multi-contrast 3D X-ray imaging of porous and composite materials, *Appl. Phys. Lett.* 106 (2015) 154102, <https://doi.org/10.1063/1.4918617>.
- [59] Y. Zhang, W. Verwaal, M.F.C. van de Ven, A.A. Molenaar, S.P. Wu, Using high-resolution industrial CT scan to detect the distribution of rejuvenation products in porous asphalt concrete, *Constr. Build. Mater.* 100 (2015) 1–10, <https://doi.org/10.1016/j.conbuildmat.2015.09.064>.
- [60] E. Masad, V.K. Jandhyala, N. Dasgupta, N. Somadevan, N. Shashidhar, Characterization of air void distribution in asphalt mixes using X-ray computed tomography, *J. Mater. Civ. Eng.* 14 (2002) 122–129, [https://doi.org/10.1061/\(ASCE\)0899-1561\(2002\)14:2\(122\)](https://doi.org/10.1061/(ASCE)0899-1561(2002)14:2(122)).
- [61] A. du Plessis, B.J. Olawuyi, W.P. Boshoff, S.G. le Roux, Simple and fast porosity analysis of concrete using X-ray computed tomography, *Mater. Struct.* 49 (2016) 553–562, <https://doi.org/10.1617/s11527-014-0519-9>.
- [62] S. Tang, C. Ramseyer, P. Samant, L. Xiang, X-ray-induced acoustic computed tomography of concrete infrastructure, *Appl. Phys. Lett.* 112 (2018) 063504, <https://doi.org/10.1063/1.5009936>.
- [63] O. Büyükoztürk, Imaging of concrete structures, *NDT & E Int.* 31 (1998) 233–243, [https://doi.org/10.1016/S0963-8695\(98\)00012-7](https://doi.org/10.1016/S0963-8695(98)00012-7).
- [64] A. Garbacz, Application of stress based NDT methods for concrete repair bond quality control, *Bull. Polish Acad. Sci. Tech. Sci.* 63 (2015) 77–85, <https://doi.org/10.1515/bpasts-2015-0009>.
- [65] F. Khan, S. Rajaram, P.A. Vanniamparambil, M. Bolhassani, A. Hamid, A. Kontsos, I. Bartoli, Multi-sensing NDT for damage assessment of concrete masonry walls, *Structural Control and Health Monitoring* 22 (n.d.) 449–462, <https://doi.org/10.1002/stc.1680>.
- [66] A.Q. Bauer, R.E. Nothdurft, J.P. Culver, T.N. Erpelding, L.V. Wang, Quantitative photoacoustic imaging: correcting for heterogeneous light fluence distributions using diffuse optical tomography, *JBO, JBOPFO.* 16 (2011) 096016, <https://doi.org/10.1117/1.3626212>.
- [67] B.T. Cox, S.R. Arridge, K.P. Köstli, P.C. Beard, Two-dimensional quantitative photoacoustic image reconstruction of absorption distributions in scattering media by use of a simple iterative method, *Appl. Opt.* 45 (2006) 1866, <https://doi.org/10.1364/AO.45.001866>.
- [68] Z. Yuan, H. Jiang, Quantitative photoacoustic tomography: recovery of optical absorption coefficient maps of heterogeneous media, *Appl. Phys. Lett.* 88 (2006) 231101, <https://doi.org/10.1063/1.2209883>.
- [69] A. Rosenthal, D. Razansky, V. Ntziachristos, Fast semi-analytical model-based acoustic inversion for quantitative optoacoustic tomography, *IEEE Trans. Med. Imaging* 29 (2010) 1275–1285, <https://doi.org/10.1109/TMI.2010.2044584>.
- [70] M.-C. Vozenin, P.D. Fornel, K. Petersson, V. Favaudon, M. Jaccard, J.-F. Germond, B. Petit, M. Burki, G. Ferrand, D. Patin, H. Bouchaab, M. Ozsahin, F. Bochud, C. Bailat, P. Devauchelle, J. Bourhis, The advantage of FLASH radiotherapy confirmed in mini-pig and cat-cancer patients, *Clin. Cancer Res.* 25 (2019) 35–42, <https://doi.org/10.1158/1078-0432.CCR-17-3375>.
- [71] J. Bourhis, W.J. Sozzi, P.G. Jorge, O. Gaide, C. Bailat, F. Duclos, D. Patin, M. Ozsahin, F. Bochud, J.-F. Germond, R. Moeckli, M.-C. Vozenin, Treatment of a first patient with FLASH-radiotherapy, *Radiother. Oncol.* 139 (2019) 18–22, <https://doi.org/10.1016/j.radonc.2019.06.019>.
- [72] V. Favaudon, L. Caplier, V. Monceau, F. Pouzoulet, M. Sayarath, C. Fouillade, M.-F. Poupon, I. Brito, P. Hupé, J. Bourhis, J. Hall, J.-J. Fontaine, M.-C. Vozenin, Ultrahigh dose-rate FLASH irradiation increases the differential response between normal and tumor tissue in mice, *Sci. Transl. Med.* 6 (2014), <https://doi.org/10.1126/scitranslmed.3008973> 245ra93–245ra93.
- [73] M. Durante, E. Bräuer-Krisch, M. Hill, Faster and safer? FLASH ultra-high dose rate in radiotherapy, *BJR.* 91 (2017) 20170628, <https://doi.org/10.1259/bjr.20170628>.
- [74] J. Bourhis, P. Montay-Gruel, P. Gonçalves Jorge, C. Bailat, B. Petit, J. Ollivier, W. Jeanneret-Sozzi, M. Ozsahin, F. Bochud, R. Moeckli, J.-F. Germond, M.-C. Vozenin, Clinical translation of FLASH radiotherapy: Why and how? *Radiother. Oncol.* 139 (2019) 11–17, <https://doi.org/10.1016/j.radonc.2019.04.008>.
- [75] P. Montay-Gruel, A. Bouchet, M. Jaccard, D. Patin, R. Serduc, W. Aim, K. Petersson, B. Petit, C. Bailat, J. Bourhis, E. Bräuer-Krisch, M.-C. Vozenin, X-rays can trigger the FLASH effect: ultra-high dose-rate synchrotron light source prevents normal brain injury after whole brain irradiation in mice, *Radiother. Oncol.* 129 (2018) 582–588, <https://doi.org/10.1016/j.radonc.2018.08.016>.
- [76] K.J. Harrington, Ultrahigh dose-rate radiotherapy: next steps for FLASH-RT, *Clin. Cancer Res.* 25 (2019) 3–5, <https://doi.org/10.1158/1078-0432.CCR-18-1796>.
- [77] M.-C. Vozenin, J.H. Hendry, C.L. Limoli, Biological benefits of ultra-high dose rate FLASH radiotherapy: sleeping beauty awoken, *Clin. Oncol.* 31 (2019) 407–415, <https://doi.org/10.1016/j.clon.2019.04.001>.
- [78] P. Montay-Gruel, M.M. Acharya, K. Petersson, L. Alikhani, C. Yakkala, B.D. Allen, J. Ollivier, B. Petit, P.G. Jorge, A.R. Syage, T.A. Nguyen, A.A.D. Baddour, C. Lu, P. Singh, R. Moeckli, F. Bochud, J.-F. Germond, P. Froidevaux, C. Bailat, J. Bourhis, M.-C. Vozenin, C.L. Limoli, Long-term neurocognitive benefits of FLASH radiotherapy driven by reduced reactive oxygen species, *PNAS* 116 (2019) 10943–10951, <https://doi.org/10.1073/pnas.1901777116>.
- [79] F. Forghani, A. Mahl, T.J. Patton, B.L. Jones, M.A. Borden, D.C. Westerly, C. Altunbas, M. Miften, D.H. Thomas, Simulation of x-ray-induced acoustic imaging for absolute dosimetry: Accuracy of image reconstruction methods, *Medical Physics* n/a (n.d.), <https://doi.org/10.1002/mp.13961>.
- [80] Sarah K. Patch, E.M. Hoff Daniel, Tyler B. Webb, G. Sobotka Lee, Tianyu Zhao, Two-stage ionoacoustic range verification leveraging Monte Carlo and acoustic simulations to stably account for tissue inhomogeneity and accelerator-specific time structure – a simulation study, *Med. Phys.* 45 (2018) 783–793, <https://doi.org/10.1002/mp.12681>.
- [81] S. Tang, D.H. Nguyen, A. Zarafshani, C. Ramseyer, B. Zheng, H. Liu, L. Xiang, X-ray-induced acoustic computed tomography with an ultrasound transducer ring-array, *Appl. Phys. Lett.* 110 (2017) 103504, <https://doi.org/10.1063/1.4978049>.
- [82] H.-P. Brecht, R. Su, M. Fronheiser, S.A. Ermilov, A. Conjusteau, A.A. Oraevsky, Whole-body three-dimensional optoacoustic tomography system for small animals, *J. Biomed. Opt.* 14 (2009) 064007, <https://doi.org/10.1117/1.3259361>.
- [83] A.A. Oraevsky, B. Clingman, J. Zalev, A.T. Stavros, W.T. Yang, J.R. Parikh, Clinical optoacoustic imaging combined with ultrasound for coregistered functional and anatomical mapping of breast tumors, *Photoacoustics* 12 (2018) 30–45, <https://doi.org/10.1016/j.pacs.2018.08.003>.
- [84] V.G. Andreev, A.A. Karabutov, S.V. Solomatina, E.V. Savateeva, V. Aleinikov, Y.V. Zhulina, R.D. Fleming, A.A. Oraevsky, Optoacoustic tomography of breast cancer with arc-array transducer, in: *Biomedical Photoacoustics*, Int. Soc. Opt. Photon. (2000) 36–47, <https://doi.org/10.1117/12.386339>.
- [85] R. Liu, L. Xiang, D. Xing, J. Li, H. Qin, W. Zhang, S. Yang, Large depth focus-tunable photoacoustic tomography based on clinical ultrasound array transducer, *Appl. Phys. Lett.* 113 (2018) 141102, <https://doi.org/10.1063/1.5040565>.

- [86] D.R.T. Sampaio, J.H. Uliana, A.A.O. Carneiro, J.F. Pavoni, T.Z. Pavan, L.F. Borges, X-ray acoustic imaging for external beam radiation therapy dosimetry using a commercial ultrasound scanner, 2015 IEEE International Ultrasonics Symposium (IUS) (2015) 1–4, <https://doi.org/10.1109/ULTSYM.2015.0400>.
- [87] S. Hickling, M. Hobson, I.E. Naqa, Characterization of x-ray acoustic computed tomography for applications in radiotherapy dosimetry, IEEE Trans. Radiat. Plasma Med. Sci. PP (2018), <https://doi.org/10.1109/TRPMS.2018.2801724> 1–1.
- [88] J. Kim, E.Y. Park, Y. Jung, B.C. Kim, J.H. Kim, C.Y. Yi, I.J. Kim, C. Kim, X-ray acoustic-based dosimetry using a focused ultrasound transducer and a medical linear accelerator, IEEE Trans. Radiat. Plasma Med. Sci. 1 (2017) 534–540, <https://doi.org/10.1109/TRPMS.2017.2757484>.
- [89] H. Lei, W. Zhang, I. Oraiqat, I.E. Naqa, X. Wang, 2D x-ray dosimetry monitoring during radiotherapy using x-ray acoustic computed tomography (Conference presentation), Photons Plus Ultrasound: Imaging and Sensing 2018, International Society for Optics and Photonics (2018) 104940F, <https://doi.org/10.1117/12.2289113>.
- [90] S. Tang, K. Yang, Y. Chen, L. Xiang, X-ray induced acoustic computed tomography for 3D breast imaging: a simulation study, Med. Phys. (2018), <https://doi.org/10.1002/mp.12829>.
- [91] S. Tang, L. Ren, P. Samant, J. Chen, H. Liu, L. Xiang, Sub-mSV breast XACT scanner: concept and design, Medical Imaging 2016: Ultrasonic Imaging and Tomography, International Society for Optics and Photonics (2016), <https://doi.org/10.1117/12.2211079> p. 97900L.
- [92] L. Xiang, S. Tang, M. Ahmad, L. Xing, XACT: A Novel Imaging Technique for Radiation Therapy Guidance, Int. J. Radiat. Oncol. Biol. Phys. 96 (2016) E654–E655, <https://doi.org/10.1016/j.ijrobp.2016.06.2268>.
- [93] H. Lei, W. Zhang, I. Oraiqat, Z. Liu, J. Ni, X. Wang, I.E. Naqa, Toward in vivo dosimetry in external beam radiotherapy using x-ray acoustic computed tomography: A soft-tissue phantom study validation, Medical Physics. 0 (n.d.), <https://doi.org/10.1002/mp.13070>.
- [94] S. Tang, K. Yang, Y. Chen, L. Xiang, X-ray induced acoustic computed tomography for 3D breast imaging: a simulation study, Med. Phys. (2018), <https://doi.org/10.1002/mp.12829>.
- [95] K. Wang, R. Su, A.A. Oraevsky, M.A. Anastasio, Investigation of iterative image reconstruction in three-dimensional optoacoustic tomography, Phys. Med. Biol. 57 (2012) 5399–5423, <https://doi.org/10.1088/0031-9155/57/17/5399>.
- [96] C. Huang, K. Wang, L. Nie, L.V. Wang, M.A. Anastasio, Full-wave iterative image reconstruction in photoacoustic tomography with acoustically inhomogeneous media, IEEE Trans. Med. Imaging 32 (2013) 1097–1110, <https://doi.org/10.1109/TMI.2013.2254496>.
- [97] C. Huang, L. Nie, R.W. Schoonover, L.V. Wang, M.A. Anastasio, Photoacoustic computed tomography correcting for heterogeneity and attenuation, JBO 17 (2012) 061211, <https://doi.org/10.1117/1.JBO.17.6.061211>.
- [98] B.T. Cox, S. Kara, S.R. Arridge, P.C. Beard, k-space propagation models for acoustically heterogeneous media: application to biomedical photoacoustics, J. Acoust. Soc. Am. 121 (2007) 3453–3464, <https://doi.org/10.1121/1.2717409>.
- [99] B.E. Treeby, J. Jaros, B.T. Cox, Advanced photoacoustic image reconstruction using the k-wave toolbox, Photons Plus Ultrasound: Imaging and Sensing 2016, International Society for Optics and Photonics (2016) 97082P, <https://doi.org/10.1117/12.2209254>.
- [100] Z. Yuan, H. Jiang, Quantitative photoacoustic tomography: recovery of optical absorption coefficient maps of heterogeneous media, Appl. Phys. Lett. 88 (2006) 231101, <https://doi.org/10.1063/1.2209883>.
- [101] T. Tarvainen, B.T. Cox, J.P. Kaipio, S.R. Arridge, Reconstructing absorption and scattering distributions in quantitative photoacoustic tomography, Inverse Probl. 28 (2012) 084009, <https://doi.org/10.1088/0266-5611/28/8/084009>.



**Pratik Samant** is a Postdoctoral Researcher in the Department of Oncology at the University of Oxford. He obtained his PhD from the University of Oklahoma within the Stephenson School of Biomedical Engineering being advised by Dr. Liangzhong Xiang. He is a co-inventor of x-ray induced acoustic computed tomography (US20180344167A1) and Nanoscale Photoacoustic Tomography (US20190170695A1).



**Luis Mario Trevisi** is an Undergraduate researcher in Chemical, Biological and Material Engineering at the University of Oklahoma. He completed the international baccalaureate program at the United World College. He assists the TRUE lab with research in Photoacoustic Microscopy (PAM), X-ray Acoustic Computed Tomography (XACT) and Proton-Induced acoustic imaging (PAI).



**Xuanrong Ji** is a professor and executive vice dean in the College of Electromechanical Engineering at Guangdong University of Technology, where he is also the Director of Ultrasound Inspection and Monitoring Lab. He is the co-founder of Doppler Electronic Technologies, Co., a leading ultrasound technology company in China. Dr. Ji is the PI of the National Major Research Instrument and Equipment Development Project from MOST, and Guangdong Innovative and Entrepreneurial Research Team Program, and National Science Foundation Grant, etc. He received the First prize of science and technology progress from China Association of Special Equipment Inspection. He has served as a chairman of ultrasound transducer and material academic committee in China Association of Medical Equipment.



**Liangzhong Xiang** is an assistant professor in the school of electrical and computer engineering at the University of Oklahoma, where he is also the Director of the TRUE Lab. His laboratory was the first to report X-ray-induced acoustic computed tomography (XACT), fast proton-induced acoustic imaging (PAI), and electroacoustic tomography (EAT). Dr. Xiang received the NIH MERIT Award (R37), and the Research Scholar Award from the American Cancer Society. He also received the Nancy L. Mergler Faculty Mentor Award in 2017 and was nominated for 2019 OU Presidential Professorships. He has served as Conference Chairs in the AAPM annual meeting in 2019 and the International Conference on Information Optics and Photonics (CIOP 2018), the SPIE Student Chapter Advisor, Associate Editor of Medical Physics journal, and Grant Reviewer for NIH, DOE, Russian Science Foundation.